Journal of
Advanced Civil and Environmental Engineering
Vol.7, No.1, 2024, pp 48-64
ISSN: 2599-3356
DOI: http://dx.doi.org/10.30659/jacee.7.1.48-64

Utilization of Buton Asphalt Solid Waste (ASW) Waste Bitumen Extraction In Concrete

Siti Aja Aulia[1] and Januarti Jaya Ekaputri[1*]

[2] *Civil Engineering Program, Faculty of Civil Planning and Geo Engineering (FTSPK), Sepuluh Nopember Institute of Technology ITS Campus, Sukolilo, Surabaya 60111, East Java*
* *Corresponding author:* januarti@ce.its.ac.id

(**Received:** May 28th, 2024 ; **Revised:** June 10th, 2024 ; **Accepted:** June 13th, 2024)

Abstract: Indonesia has 650 million tons of Buton Rock Asphalt (Asbuton) deposits. The mineral residue, known as Asphalt Solid Waste (ASW). The extraction left ASW by 65-90% of asbuton's weight. However, 770 thousand tons/year of ASW remain underutilized, causing environmental pollution due to its hydrocarbon content. Based on XRD results, Asbuton minerals were dominated with 46% $CaCO_3$, which are potential as a subtitute material in concrete. However, its hydrocarbon content at 68,911 ppm raises concerns. To prevent ASW hydrocarbons from contaminating concrete, solidification was attempted. This study investigates solidification by making Artificial Coarse Aggregate (ACA) products and using ASW as a subtitute for gravel in concrete. The ACAs were produced from a mixture of ASW and cement, molded into 50 x 100 mm cylinders, crushed after twenty eight-days moist curing, and tested according to ASTM C33 standard of gravel. ASW replaced 0-12.5% by volume of sand and ACA replaced 0-12.5% by volume of gravel in concrete with a target compressive strength of 45 MPa at twenty eight-days. Heat of hydration and shrinkage were tested to indentify the impact of $CaCO_3$ from ASW on concrete. The results showed that ACA could reduce 9% of ASW hydrocarbons. However, the ACA produced did not meet the gravel standard in ASTM because ACA absorption reached 6.75% and abrasion test up to 57%. Neverthless, ASW's high absorption reduced heat hydration by 10% and shrinkage by 83% compared to normal concrete.

Keywords: Asphalt Solid Waste; Hydrocarbon; Artificial Aggregate; Green Concrete; Internal Curing Effect

1. Introduction

Buton Island, Indonesia contains 650 milion tons of asphalt contained natural rock [1]. Buton Rock Asphalt (Asbuton) is used as an alternative material to replace petroleum asphalt by separating bitumen and minerals. The separation process is carried out in various ways, including: milling process by gravity [2], centrifugation [3], and extraction [4]. Extraction is the most widely used process due to its flexibility in adjusting it different asbuton condition. However, the disadvantage of this process is that it leaves hydrocarbon in the waste.

The Asbuton extraction process separates 10-35% of bitumen [1] with 65-90% minerals. Wika bitumen (2021) [5] targets to fulfill the asphalt Buton needs to reach 500 thousand tons per year. When fulfillment can be achieved, it creates 1.5 million for two years. For ease of identification, solid waste from extraction bitumen called as Asphalt Solid Waste (ASW).

Previous research has investigated the use of hydrocarbon materials, including: crude oil contamination replacing fine aggregate by volume in concrete [6], the kerosene contamination of concrete fine aggregate [7], and light crude oil contamination in the dry weight of concrete fine aggregates [8]. Based on these literatures, the maximum hydrocarbon content in concrete is 1% because exceeding this percentage can result in a decrease in the mechanical properties of concrete.

In guidelines for the utilization of asbuton [9], 86% $CaCO_3$ is the dominant mineral on ASW. $CaCO_3$ causes high water absorption [10] thus potentially reducing shrinkage in concrete [11]. The existence of this compound, gives hope that ASW has the potential to be used in concrete.

However, the absence of research addressing the utilization of ASW in concrete has limited the necessary information, such as the maximum limit for use of hydrocarbon-containing materials in concrete. Hydrocarbons in concrete can cause a decrease concrete mechanical properties [12]. For this reason, a solidification process of hydrocarbons is needed so as not to contaminate the concrete. One of the efforts is the manufacture of Artificial Coarse Aggeragate (ACA).

Several studies on hydrocarbon solidification have been conducted. Ahmad, et. al [13] consolidated diesel and crude oil contaminated materials using Portland Cement, concluding that 18% of TPH decreased when consolidated using 8% OPC. This shows that cement is able to inhibit and reduce hydrocarbon leaking the waste [14]. Thus, the solidification method could maximize the use of waste hydrocarbons [15].

This study aims to deal with avoid waste dumping of hydrocarbon materials. ASW is used as a replacement sand and ASW products in the form of ACA as replacement material for gravel in concrete. Compressive strength of concrete was carried out in 45 MPa. 5-12.5% ASW and ACA was replaced sand and gravel by volume. Seven variations was tested compressive strength on seven and twenty eight-days after moist curing. Total Petroleum Hydrocarbon (TPH) and Toxicity Characteristic Leaching Procedure (TCLP) were used to identify the hazardous status of ASW, ACA, and waste substitution concrete.

2. Literature Review

Quality standards of waste are determined by several regulations. A waste is analyzed for its material composition whether it contains Hazardous and Toxic Materials (known as Bahan Berbahaya dan Beracun in Indonesian (B3 status)) [16]. In the appendix XI of Goverment Regulation No. 22 of 2021 [16] contains a list of quality standards for polluting substances. There are a number of polluting substances for determining the category of B3 waste: inorganic, anion, organic, and pesticide. Each pollutant is divided into several parameters. Eleven parameters were used to determine the category of hazardous waste, which are presented on Table 1. The selection of these parameters is based on the toxic properties and environmental pollution potential of the chemicals if released into it.

Table 1. Quality Standards for TCLP Testing Parameters

Parameters (mg/L)	Quality Standard*)		
	TCLP A	TCLP B	TCLP C
Boron (B)	150.00	25.00	10.00
Cadmium (Cd)	0.90	0.15	0.06
Chromium (Cr)	15.00	2.50	1.00
Copper (Cu)	60.00	10.00	4.00
Lead (Pb)	3.00	0.50	0.20
Silver (Ag)	40.00	5.00	2.00
Zinc (Zn)	300.00	50.00	20.00
Cyanide (CN)	21.00	3.50	1.40
Fluoride (F)	450.00	75.00	30.00

Parameters (mg/L)	**Quality Standard*)**		
	TCLP A	**TCLP B**	**TCLP C**
Nitrate (NO_3)	15000	2500	1000
Nitrite (NO_2)	900.00	150.00	60.00

Goverment Regulation No. 101 of 2014 [17] Annex 1 added that hydrocarbon-contaminated waste is calssified as potentially hazardous waste. The TPH levels, as clarified in Goverment Regulation No. 128 of 2003 [18], indicate that the waste could be used if the TPH concentration is less than 10,000 ppm, or 1.00%. More than limit, the waste must be further treated.

3. MATERIALS AND METHODS

3.1. Materials

3.1.1. Cement

The cement used on this research is Gresik Portland Composite Cement (PCC), which is adjusted to the standard in Indonesian National Standard No. 7064 of 2014 [19] with a specific gravity of 3,150 kg/m^3.

3.1.2. Water

Clean water is used to hydrate cement, hardening of mortar and concrete (refer to ASTM C1602 [20]).

3.1.3. Superplasticizer (SP)

Consol P100 ESP, superplasticizer was produced by PT. Kimia Konstruksi Indonesia. The level of superplasticizer in ACA and concrete was determined based on the research trial process.

3.1.4. Natural Aggregates

sand (natural fine aggregate) with a maximum size of 5 mm [21] was used. Lumajang sand, with a specific gravity of 2,480 kg/m^3, and gravel (natural coarse aggregate) with a maximum size of 20 mm and a specific gravity of 2,600 kg/m^3 were also utilized. Before used, sand and gravel must be in Saturated Surface Dry (SSD) condition.

3.1.5. Asphalt Solid Waste (ASW)

This study used ASW derived from Buton bitumen extraction waste by the Departement of Chemical Engineering, Sepuluh Nopember Institute of Technology in collaboration with PT. Wijaya Karya Bitumen. Visual of ASW is shown on Fig. 1.

Fig. 1. Asphalt Solid Waste (ASW)

3.2. Methods

3.2.1. Mortar Sample

In this study, ASW was used as a filler by replacing sand by weight. The effect of ASW on sand and cement paste was examined in terms of mortar compressive strength response. Composition of mortar mix refers to ASTM C1602 [22]. ASW was substituted 0-100% by weight of sand (M0-

M100). SP was used at 0.70% by weight of cement. The mix composition is shown in Table 2. All mortar variations must meet the flow table diameter requirement of 200-210 mm according to ASTM C230 [23]. If the flowability did not reach this diameter, additional water was added during the mixing process. The compressive strength was tested at fourteen and twenty eight-days after moist curing.

Table 2. Composition of Substitution Mortar Mix

Mortar Variation	**Material (kg/m^3)**				
	Cement	Water	SP	Sand	ASW
M0	666	323	4.7	1,833	0
M20	666	323	4.7	1,466	367
M30	666	353	4.7	1,283	550
M40	666	400	4.7	1,100	733
M50	666	446	4.7	917	917
M60	666	493	4.7	733	1,100
M70	666	540	4.7	550	1,283
M80	666	600	4.7	367	1,466
M90	666	660	4.7	183	1,650
M100	666	660	4.7	0	1,833

3.2.2. Production of Artificial Coarse Aggregate (ACA)

The maximum utilization of waste was achieved with 100% ASW. However, a high percentage of ASW resulted in high hydrocarbon content as well. Therefore, the solution was to utilize 100% ASW while binding hydrocarbons to prevent contamination of other concrete components, and cement hydration was achieved through the production of ACA. The material composition of ACA referred to M100 in Table 2. Cement, water, SP, and ASW were mixed in a mixer for approximately three minutes. The mixture was poured in 3 layers into a 50 mm x 100 mm mortar cylinder mold. Each layer was troweled twenty four-times [22]. After approximately twenty four hours, the mold was opened, and each cylinder was moist cured. The cylinders were crushed in a crusher when they reached the twenty eight-days moist curing period. The ACA manufacturing method is illustrated in Fig. 2.

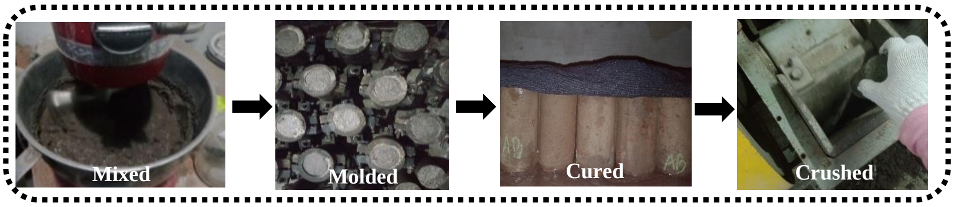

Fig. 2. ACA Manufacturing Method

ACA was generated in this section with some visual identification. ACA has a light brown color caused by the content of organic compounds in the form of hydrocarbons from the solvent (kerosene) and carbon from the remaining bitumen that remanins in the waste. ACA still smells of kerosene. The ACA product is shown in Fig. 3.

Fig. 3. Artificial Coarse Agreggate (ACA)

3.2.3. Concrete Sample Production

The production of concrete referred to ACI method [24]. Concrete variations were produced through the substitution of ASW in place of sand volume by 5%, 10%, and 12.5% (CASW). In addition, there were concrete variations made by substituting ACA for the volume of gravel by 5%, 10%, and 12.5% (CACA). All variations had to achieve a slump approximately twelve centimeters. If not achieved, an additional SP content was used. The composition of the concrete mixture is presented in Table 3. The concrete mixture was compacted in 100 mm x 200 mm cylindrical molds. The molds were opened after approximately twenty four hours and followed with moist curing treatment. All variations were tested for compressive strength at seven and twenty eight days. The impact of ASW substitution on concrete was tested for heat of hydration and autogeneous shrinkage. CASW12.5 was tested for twenty four-hours heat of hydration using a thermocouple and six-day shrinkage using an embedded strain gauge.

Table 3. Composition of Concrete Variations

Materials	**Compositions (kg/m^3)**						
	CC	**CASW5**	**CASW10**	**CASW12.5**	**CACA5**	**CACA10**	**CACA12.5**
Water	181	181	181	181	181	181	181
Sand	431	409	368	322	431	431	431
Gravel	1044	1044	1044	1044	992	940	914
ACA	0	0	0	0	29	58	72
ASW	0	12	23	27	0	0	0
Cement	600	600	600	600	600	600	600
SP	0.25%	0.26%	0.29%	0.33%	0.25%	0.25%	0.25%

3.2.4. Mixing Sequence Procedure

This section was conducted to analyze effect of ASW mixing sequence on hydrocarbon content through twenty eight-days mortar compressive strength testing and TPH testing. Two mixing methods were applied to the mortar mix, ASW was mixed at the earliest (Q1) and latest (Q2) times. Methods Q1 and Q2 are shown in Fig. 4.

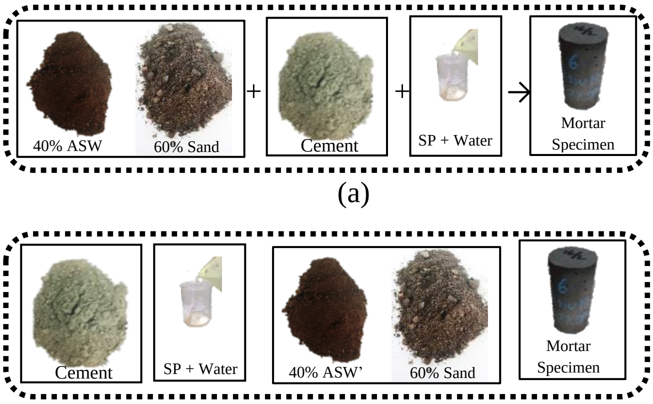

(b)

Fig. 4. Mixing Sequence (a) MQ1 (b) MQ2

4. Results and Discussion

4.1. Asphalt Solid Waste Characterizations

Quality standard parameters in Table 1 adjusted it the results of the TCLP ASW parameters analysis in Table 4. In Table 1 and Table 4, all TCLP parameters in ASW are below the standard requirement. This indicates that ASW is not classified as hazardous waste. Based on the TPH results in Table 4, the hydrocarbon content in ASW is 6.89%. These hydrocarbon levels must be reduced until the TPH is less than 10,000 ppm. Therefore, the ASW treatment process is required.

Table 4. TCLP and TPH Testing on ASW

Parameters	Analysis Result
Boron (B)	1.34 mg/L
Cadmium (Cd)	0.00 mg/L
Chromium (Cr)	0.05 mg/L
Copper (Cu)	0.00 mg/L
Lead (Pb)	0.04 mg/L
Silver (Ag)	0.03 mg/L
Zinc (Zn)	9.67 mg/L
Cyanide (CN)	0.00 mg/L
Fluoride (F)	4.63 mg/L
Nitrate (NO_3)	0.45 mg/L
Nitrite (NO_2)	0.01 mg/L
TPH	68,912 ppm

X-Ray Fluorosence (XRF), X-Ray Diffraction (XRD), and Scanning electron Microscope (SEM) were used to identify the chemical composition, phase changes, and microstructure of ASW as a substitute material with effect on concrete. The chemical compsosition and Loss On Ignition (LOI) are shown in Table 5. Table 5 shows the main oxides of ASW are CaO, SiO_2, Al_2O_3, MgO, and Fe_2O_3. LOI defined by ACI 116 [25] is the percentage mass loss of a sample burned at a specified temperature to a fixed weight, typically between 900°C – 1,000°C. LOI is used as an indicator to determine the level of organic carbon in the material. High LOI in ASW is related to presence of combustible organic content. This can lead to discoloration, and segregation of the concrete [26]. Atis [27] found that LOI increases the water demand of fresh concrete. High carbon content provides one source of high LOI and is believed to interfere with the hydration reaction in cement.

Table 5. Chemical Composition and Loss on Ignition of ASW

Chemical Groups	Name	Unit
CaO	Calcium Oxide	33.71%
SiO_2	Silicon Dioxide	13.82%
Fe_2O_3	Iron (III) Oxide	2.58%
SO_3	Sulfur Trioxide	3.44%
Al_2O_3	Aluminium Oxide	3.49%
K_2O	Potassium Oxide	0.43%
TiO_2	Titanium Dioxide	0.23%
MgO	Magnesium Oxide	3.39%
Na_2O	Sodium Oxide	0.46%
LOI	Loss On Ignition	38.05%

The mineral content and mineral percentage of ASW are shown in Fig. 5 and Table 6. The XRD analysis of ASW shows that 63.72% of the minerals are amorphous. Amorphous materials require a stabilizing position. This enables the material to form new crystals when it binds with cement.

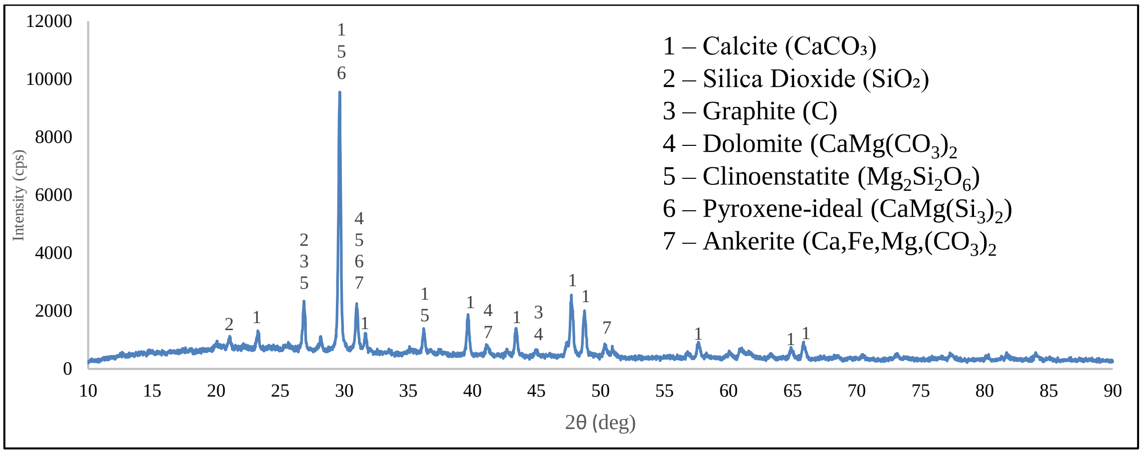

Fig. 5. XRD of ASW

Table 6. Mineral Composition of ASW from XRD Result

Minerals	Composition Group	Percentage (%)
Calcite	$CaCO_3$	46.10
Silicon Oxide (Quartz)	SiO_2	17.20
Graphite	C	11.40
Dolomite	$CaMg(CO_3)_2$	9.50
Clinoentatite	$Mg_2Si_2O_6$	9.30
Pyroxene-ideal	$CaMg(SiO_3)_2$	6.00
Ankerite	Ca, Fe, Mg $(CO_3)_2$	0.60
Degree Of Cristalizations (DOC)		36.28
Amorphous		63.72

$CaCO_3$ is the dominant mineral in ASW. Fig. 6 is the ASW observed through SEM. The figure shows that the ASW particles are agglomerated irregulars less than 3 µm in size. Magnesium calcite and calcite in cement mortars result in a significant increase in compressive strength, especially at the beginning of hardening, due to the acceleration of cement hydration [28].

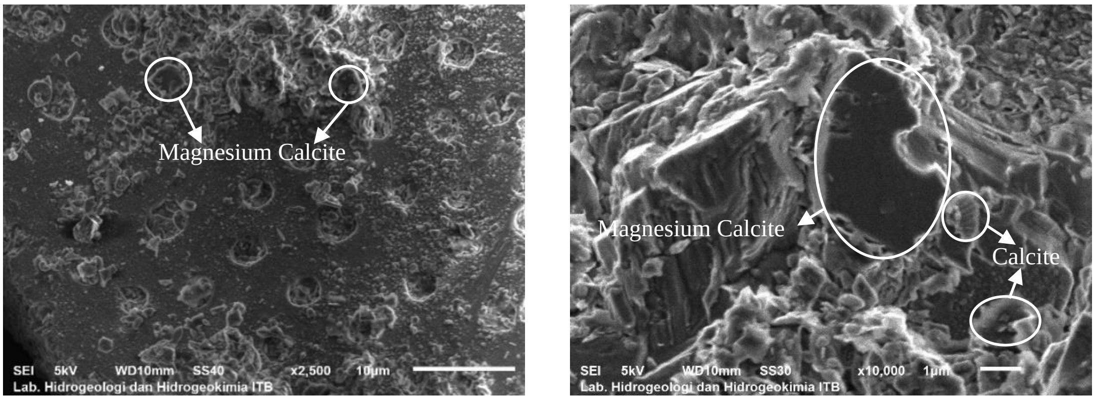

(a) (b)

Fig. 6. SEM of ASW (a) 2500x Magnification (b) 10000x Magnification

4.2. Mortar

4.2.1. Mortar Flowability

The flowtable instrument must be adjusted to reach a diameter of 200-210 mm, indicating that additional water is required as the amount of ASW in the mortar mix increases. This condition is shown in Fig. *7*. The w/c ratio of M30 increased by 8.5% from M20. Consistenly, M40-M70 increased by 11.7%. Even M80, M90, and M100 had almost equal amounts of cement and water (mass ratio of 1.0).

ASW is dominated by $CaCO_3$ and SiO_2. The presence of $CaCO_3$ and SiO_2 can minimize the pore space so that the mortar structure is denser [29]. When ASW is added to a mortar mix, it fills the space between cement particles. This may result in some of the water that normally adheres to the cement particles being absorbed by the $CaCO_3$ ASW. Thus, the total amount of water in the mix is distributed unevenly. This condition causes the binder particles and aggregates to move or reposition more as the flowing medium (water) is reduced. As the ASW content increase, additional water is required (w/c ratio increases) for the mixture to flow easily (flowtable achieved).

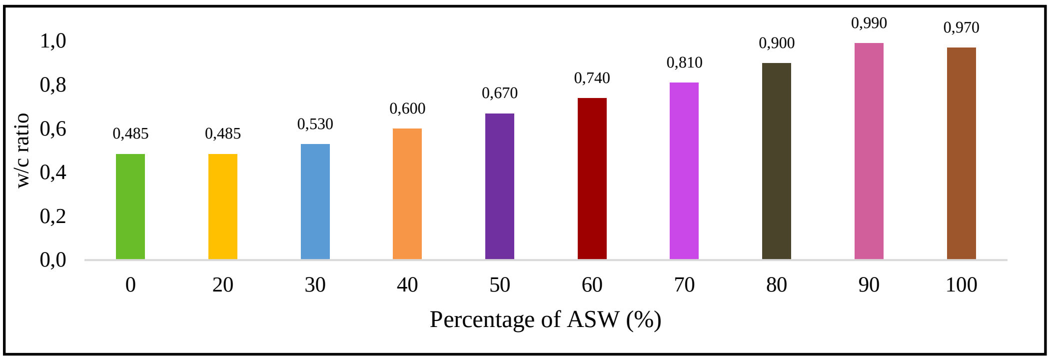

Fig. 7. W/C Ratio versus ASW Percentage in Mortar

4.2.2. Mortar Compressive Strength

Substitution of 0-100% ASW to the weight of sand resulted in significant diffrences in compressive strength, shown in Figure 8. The data results showed that 40% ASW substitution resulted in the highest compressive strength compared to the other percentage substitutions (no M0). This capability is attributed to the effect of the ASW filler, the optimal composition of the material, and the chemical interactions that foster a strong crystal structure and bond. However, the compressive strength of M40 is only half that of M0. This is due to the hydrocarbon content, which hinders the cement hydration process and tends to be insoluble in water. The product of non-optimal hydration causes the compressive strength not to reach that of control mortar.

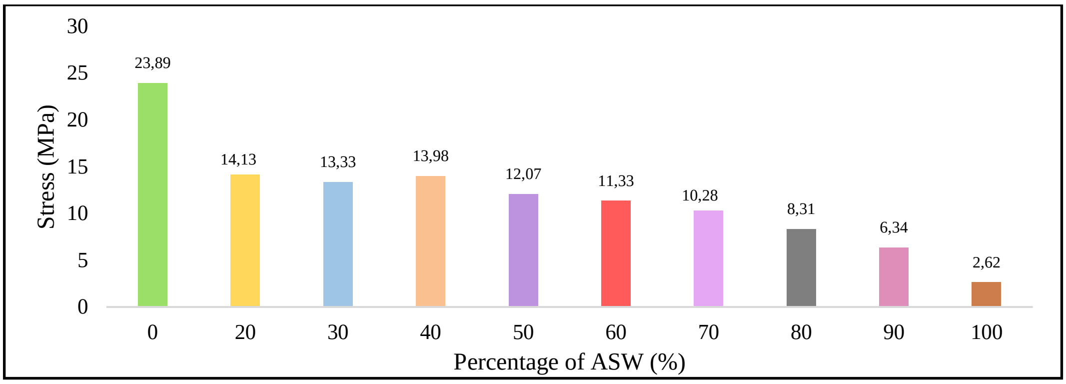

(a)

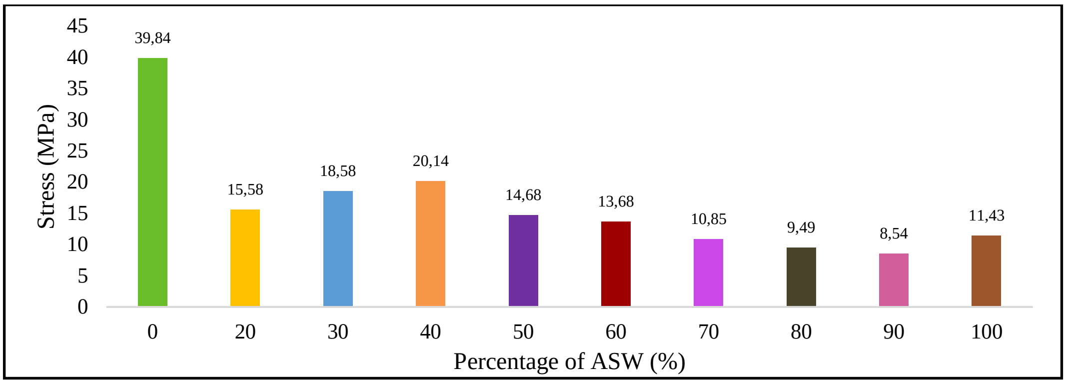

(b)

Figure 8. Compressive Strength of ASW Mortar After (a) Fourteen-Days, and (b) Twenty Eight-Days Treatment

4.2.3. Effect of Mixing Sequence on Mortar Compressive Strength

The impact of hydrocarbons during mixing is examined through the compressive strength of M40. The different mixing sequence changes the effect of hydrocarbons in ASW on compressive strength. The compressive strength of MQ2 increased by 42% over MQ1 because the hydrocarbon content of MQ1 was higher 43% than MQ2 Fig. ***9***.

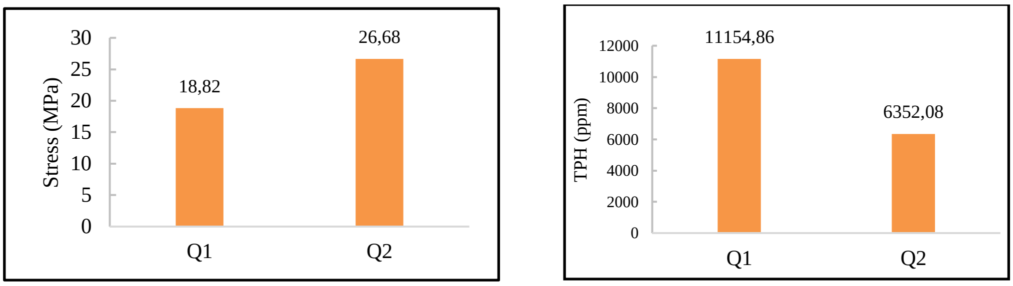

(a) (b)

Fig. 9. (a) Compressive Strengt3h (b) Total Petroleum Hydrocarbon (TPH) Mortar Mixing Order

The interaction between water, cement and ASW affects the physical and mechanical properties of mortar. ASW contains $CaCO_3$ as well as carrying hydrocarbons (oil). Water has a higher density than oil. When ASW and sand are mixed first followed by cement, the lime in the cement absorbs the oil from ASW but does not react with it. When water is added, the oil that the cement has absorbed is pushed away from the cement by the water (due to different densities). So the TPH of Q1 higher than Q2. On the other hand, the lime in ASW and cement absorbs water. Absorption of water by ASW and cement causes shrinkage in the mortar, so the compressive strength of Q1 is lower than that of Q2. In Q2, cement and water were reacted first. Then ASW was mixed into the cement paste. This condition caused $CaCO_3$ not to absorb water due to the obstruction of oil on the surface of ASW so that ASW was not involved in the chemical reaction between cement and water. However, this phenomenon makes ASW act as a filler in the mortar so that Q2 has a higher density than Q1. This result is presented in the compressive strength results in Fig. 9.(a).

4.2.4. X-Ray Diffraction (XRD) of M40 and M100

Fig. 10 shows the graph of mineral changes in the materials used to produce M40 and M100 mortars. M100 has a low quality characterized by a high percentage of $Ca(OH)_2$ and low CSH (Table 7). The high percentage of $Ca(OH)_2$ in M100 indicates an ineffective hydration reaction because the more ASW used, the more hydrocarbons in the mortar. The higher w/c ratio in M100 also plays a role in influencing the crystalline phase. An increase in w/c ratio can increase the solubility. Hydrocarbon contamination can complicate the hydration mechanism by affecting and hindering cement reactivity.

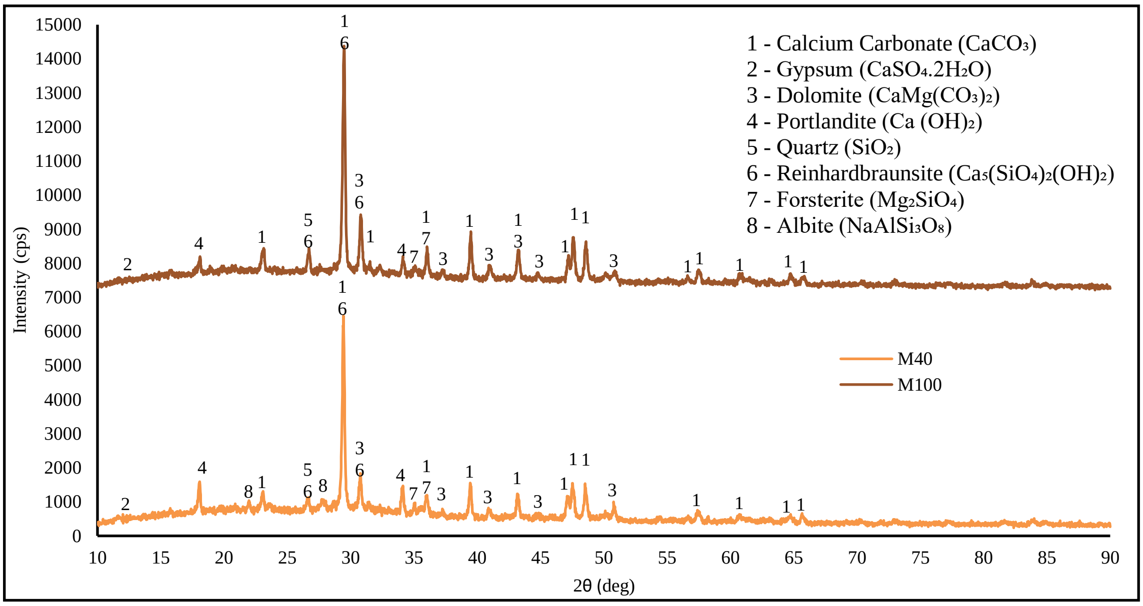

Fig. 10. XRD of M40 and M100

Table 7. Mineral Percentage of M40 and M100 Based on XRD

Symbol	Minerals	Composition Group	Percentage (%)	
			M40	**M100**
1	Calcium Carbonate	$CaCO_3$	8.234	15.851
2	Gypsum	$CaSO_4.2H_2O$	1.203	4.170
3	Dolomite	$CaMg(CO_3)_2$	5.777	2.513
4	Portlandite	$Ca (OH)_2$	0.288	1.978
5	Quartz	SiO_2	0.680	0.989
6	Reinhardbraunsite	$Ca_5(SiO_4)_2(OH)_2$	2.222	0.749
7	Forsterite	Mg_2SiO_4	4.261	0.481
8	Albite	$NaAlSi_3O_8$	3.503	-
Degree Of Cristalizations (DOC)			26.14	26.73
Amorphous			73.86	73.27

4.2.5. Scanning Electron Microscope (SEM) M40 and M100

Fig. ***11***(a) and (b) are the morphology of M40 and M100. The $CaCO_3$ in M40 has a tight structure and the hydration process is optimized so that the compressive strength of M40 is higher than other substitution variations (without M0). The hydration phase of M40 produces three times higher CSH than M100. While the structure of M100 is more porous due to the high water content (Fig. ***11***(b)).

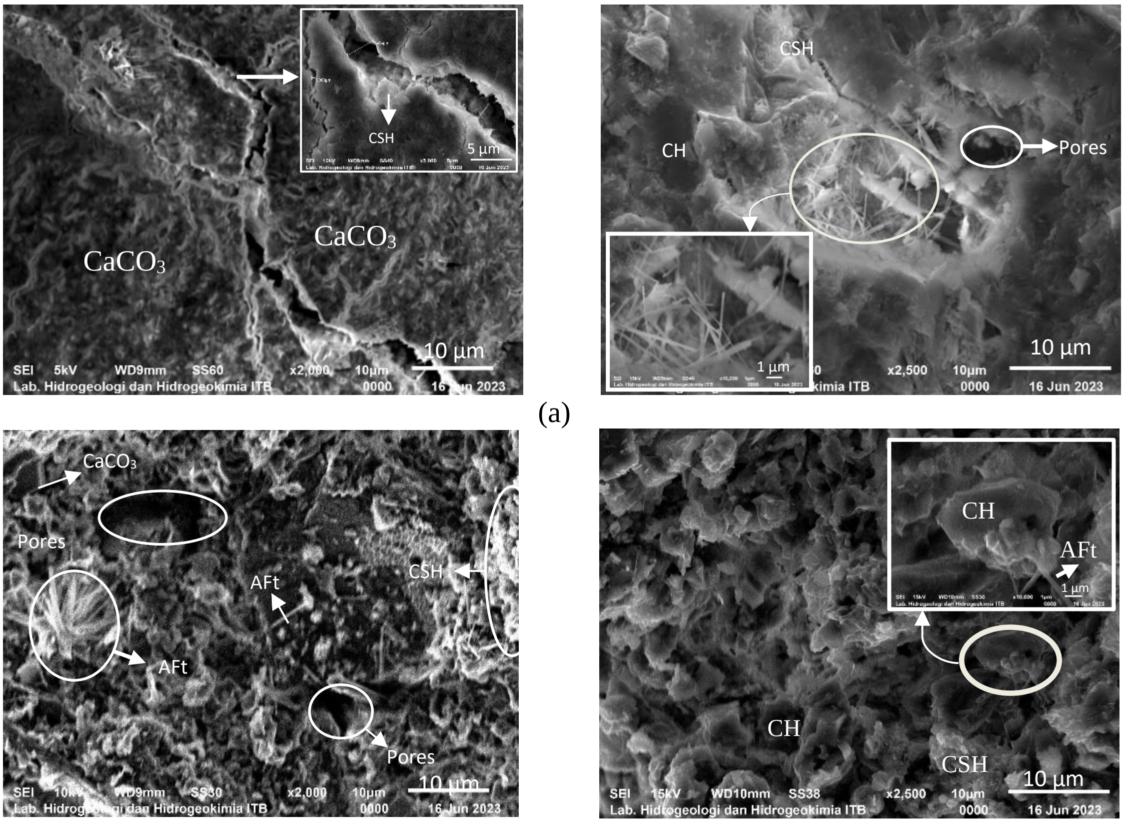

(a)

(b)

Fig. 11. SEM (a) M40 and (b) M100

The presence of excess water causes the cement particles to be spaced far apart. As a result, hydrates formed on one cement particle must travel a greater distance to reach hydrates growing on the surface of adjacent cement particles [30]. This condition is illustrated in Fig. ***12***. The surface area of the unit cell in Fig. 12(a) is

$$a \times a = a^2 \qquad (1)$$

The surafce of cement particles is

$$4 \times \tfrac{1}{4} (3{,}14 \times (\tfrac{1}{3}a)^2) = \frac{3.14}{9}a^2 \qquad (2)$$

The spesific gravity of cement particles is theoretically used 3,14. Then the mass of cement particles in a unit cell is

$$3{,}14 \times (\frac{3.14}{9}a^2) = 1.096a^2 \qquad (3)$$

The volume (and mass) of water contained in a unit cell is

$$a^2 - \frac{3.14}{9}a^2 = 0.652\, a^2 \qquad (4)$$

Therefore, the w/c ratio on the unit cell is

$$\frac{0.652\, a^2}{1.096\, a^2} = 0.594 \approx 0.60 \qquad (5)$$

Based on the linear interpolation of ACI 211.4R [24], w/c ratio of 0.60 results in a compressive strength of 28 MPa. Meanwhile, there is another cement particle of radius a (assumed to be at the center of the unit cell) with its diagonal is 1.414 Fig. 12(b). Then the minimum distance between two particles is

$$\tfrac{1}{2}(1.414a - a) = 0.207a \qquad (6)$$

Similar calculations from Eq.(1) to Eq.(5) show that the w/c ratio of this new cell is 0.207. This w/c ratio yields a compressive strength of 76 MPa (linear innterpolation from ACI 211.4R [24]).

these two conditions show that the minimum w/c ratio can produce the optimum compressive strength.

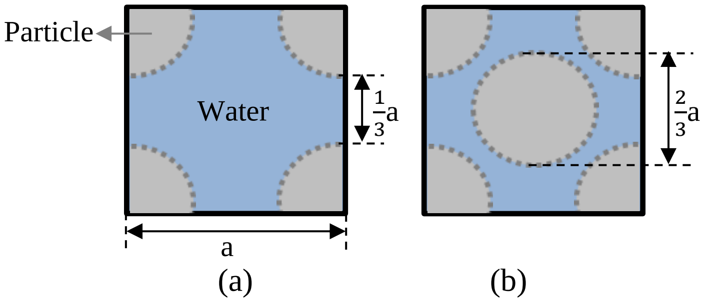

Fig. 12. 2D Illustration of the Relationship Between W/c Ratio and Distance Between Cement Particles (a) Looser System, (b) Denser System.

4.3. ACA Products

The ACA characterization test results show that the artificial coarse aggregate produced does not meet the ASTM requirements for gravel (Table 8). Too high w/c ratio causes the resulting aggregates to be too brittle, lightweight and relatively small in size. In addition, the TPH of the ASW was 63,471 ppm (Table 9). The TPH indicates that ACA is still classified as hazardous waste (B3 waste) [18]. Therefore, the use of AKB in concrete is limited to a maximum of 12.5%.

Table 8. ACA Product Characterization

Category	**Test Results**	**Defined Terms**[31]
Spesific gravity	1.42 t/m^3	1.6 – 3.3 t/m^3
Weight Volume	0.98 t/m^3	1.6 – 1.9 t/m^3
Absorbtion	6.75%	Max. 4%
Modulus of Smoothness	2.57	6.0 – 7.1
Abrasion Test	57.11%	Max. 50%

Table 9. TCLP and TPH of ASW

Parameters	**Analysis Result**
Boron (B)	2.46 mg/L
Cadmium (Cd)	0.00 mg/L
Chromium (Cr)	0.18 mg/L
Copper (Cu)	0.00 mg/L
Lead (Pb)	0.05 mg/L
Silver (Ag)	0.04 mg/L
Zinc (Zn)	12.08 mg/L
Cyanide (CN)	0.00 mg/L
Fluoride (F)	1.04 mg/L
Nitrate (NO_3)	1.07 mg/L
Nitrite (NO_2)	0.01 mg/L
TPH	63,471 ppm

4.4. Concrete

4.4.1. Compressive Strength

Comparison of compressive strength of ASW (CASW) and ACA (CACA) substituted concrete is shown in Fig. *13*. At seven days, the compressive strength of CASW5 and CACA10 was higher than CC (Fig. 13 (a)). At twenty eight days, the compressive strength of was higher than the substitution variations (CASW and CACA) (Fig. 13 (b)).

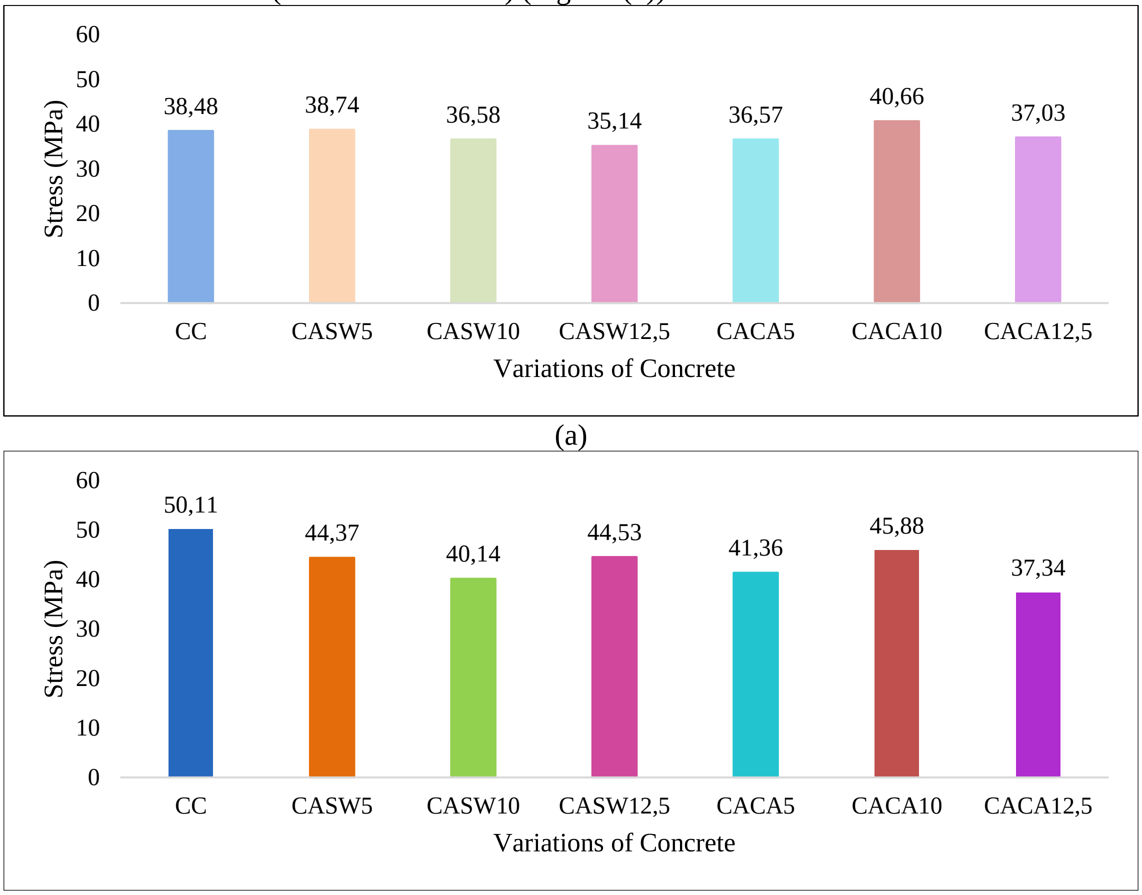

(a)

(b)

Fig. 13. Compressive Strength of Concrete Variations Aged (a) Seven-Days, and (b) Twenty Eight-Days

The hydrocarbons in ASW are first bound through cement hydration to become ACA. This process minimizes hydrocarbon contamination of the concrete. In addition, the high absorption of ACA provides internal curing to the concrete, the moisture of the concrete is maintained so that the hydration reaction can run optimally.

In concrete, ASW as a substitute for sand can be used up to 12.5%. The formation of a strong concrete structure is the bond between cement grains and aggregates. However, the presence of hydrocarbons in ASW causes the bond between grains in the concrete matrix become weak because the hydrophobic nature of hydrocarbons hinders the hydration process and inhibits the formation of hydrates.

ASW used directly (sand replacement) or pre-processed (gravel replacement) in concrete has different amounts. One cylinder of mortar before crushing can produce an average of 83% ready-mixed ASW. To produce 1 m^3 of ACA, 1,833 kg of ASW is required. Therefore, the ASW required to produce ACA is 1,528 kg/m^3. The maximum ASW in concrete is required to be 72 kg/m^3. While 12.5% ASW in concrete requires 27 kg/m^3. This means that ASW in CACA is more than ASW in CASW.

The amount of ASW in CASW and CACA affects the hydrocarbon content of the concrete. Based on the TPH test results, CASW12.5 has a TPH of 3,974 ppm and CACA12.5 has a TPH of 7,468 ppm. These results show that the hydrocarbons from 100% ASW cannot be consolidated using cement because the wear of ACA reaches 57%. Therefore, the amount of ASW used should be reduced to produce artificial coarse aggregate with wear below 50%, the w/c ratio should be minimized to make the ACA less brittle, and other solidification methods are required.

4.4.2. Heat of Hydration

Comparison of the heat of hydration was made between the 12.5% ASW substituted concrete mix (CASW12.5) and the normal concrete (CC), which were tested for twenty four-hours and presented in Fig. 14. The substitution of 12.5% ASW resulted in a concrete heat of hydration of 31.3°C, while the heat of hydration of CC was 41.2°C [32]. These two results showed that the heat of hydration of CASW12.5 was 9.9% lower than CC. The low heat of hydration in concrete indicated that the chemical reactions that occurred during the hardening process produced a limited amount of heat. The increase in ASW substitution caused more $CaCO_3$ to form. When $CaCO_3$ was excessive, the release of accumulated heat of hydration was reduced [33]. This phenomenon was due to the dispersion factor of $CaCO_3$ in water, which reduced the contact of water with C_3S [34]. The heat released by concrete did not depend on the amount of cement mixed, but on the amount of cement that was actually hydrated when the concrete was poured into the mold [30].

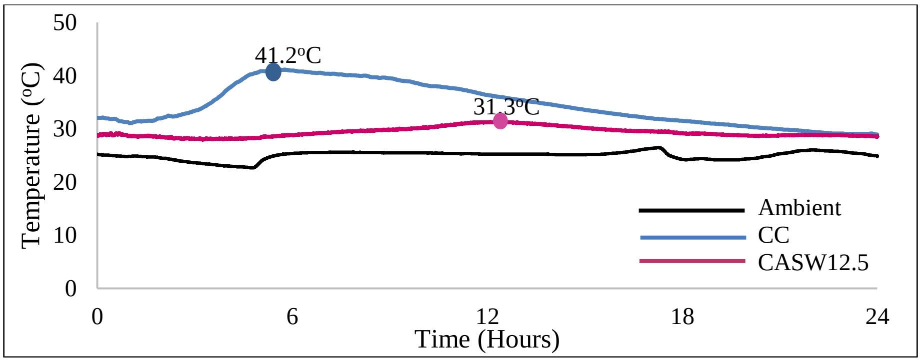

Fig. 14. Heat of Hydration

4.4.3. Shrinkage

The shrinkage test of two concrete variations were conducted for almost six-days. CC reached 470 μm [32]. Substitution of 12.5% ASW in concrete resulted in a shrinkage of 77 ($\times 10^{-6}$) which is shown in Fig. 15. This meant that ASW could reduce shrinkage by 82.89%. This was due to the activity of ASW as a filler that inhibited the reaction between AFt (ettringite) and calcium carboaluminate to form AFm, which was the mineral transformation stage of concrete [34]. When this reaction was inhibited, pore formation caused by volume shrinkage as AFt transformed into AFm was also inhibited. ASW as a filler helped to control concrete shrinkage by filling void spaces and minimizing pore formation that could cause a decrease in concrete volume.

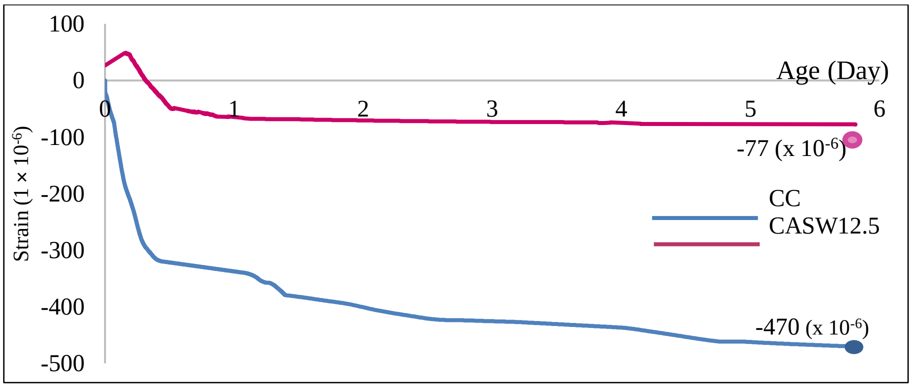

Fig. 15. Shrinkage of CASW12.5

5. Summary

The effect of hydrocarbons and $CaCO_3$ on the physical and mechanical properties of mortar, artificial aggregates, and concrete were investigated. From this study, it concluded that ASW mixed at the final stage (Q2) reduced 43% of hydrocarbons than ASW mixed at the initial stage (Q1). Hence, 42% higher compressive strength of Q2 than Q1. In addition, solidification of ASW in the form of artificial aggregates could reduce 7.3% hydrocarbon contamination of concrete or the TPH of CASW12.5 was 4,287 ppm and that of CACA12.5 was 3,974 ppm. The resulting ACA did not meet the gravel standard in ASTM because ACA absorption reached 6.75% and abrasion test up to 57%. However, the high absorption of ACA provided internal curing to the concrete, maintaining moisture content, resulting in the compressive strength of CACA substitution concrete reaching 46 MPa. The substitute concrete exhibited limited heat of hydration, resulting in a 10% reduction in heat production during the hardening process. The substitution of 12.5% ASW resulted in an 83% increase in concrete shrinkage, despite ASW's role in minimizing pore formation and maintaining concrete volume.

References

[1] Arisat., & Hendrajaya, L. (2016, 21 Mei). Fisika Pengolahan Aspal Buton. Seminar Nasional Pendidikan dan Saintek (SNPBS). Universitas Muhammadiyah Surakarta, Surakarta. ISSN: 2557-533X

[2] Imaduddin, D., & Amal, R.M. (2020). Skripsi TK184704: Studi Pemisahan Bitumen dari Asbuton Menggunakan Proses Milling dengan Penambahan Solar, Surfaktan Sodium Dedocyl Benzenesulfonat (SDBS) Dan Natrium Hidroksida (NAOH). FTIRS Institut Teknologi Sepuluh Nopember.

[3] Halimi, M., Mochtar, I. B., & Altway, A. (2014). A Breakthrough in Asphalt Tech-nology-Cheaper Bitumen Extracted from “Asbuton”, the Rock Asphalt of Buton Island, Indonesia. International Journal of Education and Research, Vol. 2, Pp. 347-358. ISSN: 2201-6740

[4] Saadah, N., Altway, A., & Rachmawati, Y. (2020). Catalytic Pyrolysis of Asbuton into Liquid Fuel with Zeolite as Catalyst. Malaysian Journal of Fundamental and Applied Science, Vol. 16, Pp. 196-200. https://doi.org/10.11113/mjfas.v16n2.1548

[5] CNBC Indonesia. (2021, 21 Februari). Wika Bitumen Targetkan Produksi Asbuton 500 Ribu Ton/Tahun. https://www.cnbcindonesia.com/market/20210218172559-19-224423/wika-bitumen-targetkan-produksi-asbuton-500-ribu-ton-tahun

[6] Ezeokpube, G.C., Alaneme, G.U., Attah, I.C., Udousoro, I.M., & Nwogbo, D. (2022). Experimental Investigation of Crude Oil Contaminated Soil for Sustainable Concrete Production. Architecture, Structures and Construction, Vol.2, Pp. 349-364 https://doi.org/10.1007/s44150-022-00069-2.

[7] Shahrabadi, H., & Vafaei, D. (2015). Effect of Kerosene Impacted Sand on Compres-sive Strength of Concrete in Different Exposure Conditions. Journal of Materials and Environmental Science, Vol.6, Pp 2665-2672 ISSN : 2028-2508

[8] Abousnina, R., Manalo, A., Lokuge, W., & Al-Jabri, K.S. (2018). Properties and Structural Behavior of Concrete Containing Fine Sand Contaminated with Light Crude Oil. Construction and Building Materials, Vol. 189, Pp 1214-1231 https://doi.org/10.1016/j.conbuildmat.2018.09.089.

[9] Departemen Pekerjaan Umum Direktorat Jenderal Bina Marga. (2006). Buku 1 Umum Pemasandatan Asbuton No: 001 – 01 / BM / 2006. Bina Marga, Jakarta.

[10] Li, W., Wang, X. C., Xiong, L., & Huang, Z. (2020, 10-12 Juli). Experimental Study on the Dry Shrinkage Properties of Nano Concrete Materials. Journal of Physics: Con-ference Series. IOP Publishing Ltd, Hangzhou. https://doi.org/10.1088/1742-6596/1605/1/012157

[11] Jiang, Y., Ling, T. C., & Shi, M. (2020). Strength Enhancement of Artificial Aggregate Prepared with Waste Concrete Powder and its Impact on Concrete Properties. Jour-nal of Cleaner Production, Vol. 257, Pp.1-9 https://doi.org/10.1016/j.jclepro.2020.120515

[12] Abbas, Z. K, I. (2017). Effect of Kerosene and Gas Oil Products on Different Types of Concrete. International Journal of Science and Research, Vol. 6, Pp.1718-1722, doi: 10.21275/ART20178987

[13] Ahmad, S., Al-Amoudi, O.S.B., Mustafa, Y.M.H., Maslehuddin, M., & Al-Malack, M., (2020). Stabilization and Solidification of Oil-Contaminated Sandy Soil Using Portland Cement and Supplementary Cementitious Materials. Journal of Materials in Civil Engineering ASCE Library, Vol. 32, Pp. 1-13 DOI: 10.1061/(ASCE)MT.1943-5533.0003169

[14] Masrullita, Burhan, R.Y.P., & Trihadiningrum, Y. (2018). Stabilization/Solidification of Waste Containing Heavy Metals and Hydrocarbons Using OPC and Land Trass Cement. Journal of Ecological Engineering, Vol. 19, Pp.88-96 https://doi.org/10.12911/22998993/92926

[15] Roslee, N.F., Kamil, N.A.F.M., Kadir, A.B., Jalil, A.R., Hamzah, N., Noor, N.M., Sandu, A.V. (2022). New Ray on Remediation of High Rings Polycyclic Aromatic Hydrocarbons: Remediation of Raw Petroleum Sludge Using Solidification and Stabilization Method. Archives of Metallurgy and Materials, Vol. 67, Pp. 1201-1208 DOI: https://doi.org/10.24425/amm.2022.141043.

[16] Peraturan Pemerintah Republik Indonesia Nomor 22 Tahun 2021. Tentang Penyelenggaraan Perlindungan dan Pengelolaan Lingkungan Hidup.

[17] Peraturan Pemerintah Republik Indonesia Nomor 101 Tahun 2014. Tentang Pengel-olaan Limbah Bahan Berbahaya Dan Beracun.

[18] Keputusan Menteri Lingkungan Hidup No. 128 Tahun 2003. Tentang Tata Cara Persyaratan Teknis Pengolahan Limbah Minyak Bumi dan Tanah Terkontaminasi Oleh Minyak Bumi Secara Biologi.

[19] Standar Nasional Indonesia Nomor 7064 Tahun 2014. Tentang Semen portland komposit.

[20] American Society for Testing and Material (ASTM) C1602. Standard Specification for Mixing Water Used in the Production of Hydraulic Cement Concrete.

[21] American Society for Testing and Material (ASTM) C33. Standard Specification for Concrete Aggregates.

[22] American Concrete Institute (ACI) 116. Cement and Concrete Terminology.

[23] American Society for Testing and Material (ASTM) C230. Standard Specification for Flow Table for Use in Tests of Hydraulic Cement

[24] American Concrete Institute (ACI) 211.4R. Guide for Selecting Proportions for High-Strength Concrete Using Portland Cement and Other Cementitious Materials. [25] "Cement and Concrete Terminology ACI 116R-00."

[26] Chusilp, N., Jaturapitakkul, C., & Kiattikomol, K. (2009). Effects Of LOI of Ground Bagasse Ash on the Compressive Strength and Sulfate Resistance of Mortars. Construction and Building Materials, 23, 3523–3531. https://doi.org/10.1016/j.conbuildmat.2009.06.046

[27] Atis, C.D. (2005). Strength Properties of High-Volume Fly Ash Roller Compacted and Workable Concrete, and Influence of Curing Condition. Cement and Concrete Research, Vol. 35, Pp. 1-10 doi:10.1016/j.cemconres.2004.07.037.

[28] Abdel-Gawwad, H.A., Heikal, M., Mohammed, M.S., El-Aleem, S.A., Hassan, H.S., Vásquez García, S.R., & Rashad, A.M. (2019). Evaluating the Impact of Nano-Magnesium Calcite Waste on the Performance of Cement Mortar in Normal and Sulfate-Rich Media. Construction and Building Materials, Vol. 203, Pp.1 https://doi.org/10.1016/j.conbuildmat.2019.01.108.

[29] Syamsunur, D., Wei, L., Ahmed Memon, Z., Surol, S., & Md Yusoff, N. I. (2022). Concrete Performance Attenuation of Mix Nano-SiO2 and Nano-CaCO3 under High Temperature: A Comprehensive Review. Materials MDPI, Vol. 15, Pp. 1-24. https://doi.org/10.3390/ma15207073

[30] Aïtcin, P.-C., & Flatt, R. J. (2016). Science and Technology of Concrete Admixtures. Elsevier, British

[31] Hamdi, F., Lapian, F.E.P., Tumpu, M., Irianto, M., Mabui, D.S.S, Raidyarto, A., Sila, A.A., Masdiana., Rangan, P.R., & Hamkah. (2021). Teknologi Beton. Tohar Media, Makassar

[32] Nurrizki, Y. (2022). Tesis RC185401: Pengaruh Removal Untuk Peningkatan Kuali-tas Low-Grade Fly Ash Pada Aplikasinya di Beton Hijau. FTSPK Institut Teknologi Sepuluh Nopember.

[33] Wu. Z, Khayat. K.H, Shi.C, Tutikian. B. F, Chen. Q. (2021). Mechanisms Underlying the Strength Enhancement of UHPC Modified with Nano-SiO_2 and Nano-$CaCO_3$. Cement and Concrete Composites, 119, Pp. 1-14. https://doi.org/10.1016/j.cemconcomp.2021.103992

[34] Fu, Q., Zhang, Z., Zhao, X., Xu, W., & Niu, D. (2022). Effect Of Nano Calcium Carbonate on Hydration Characteristics and Microstructure of Cement-Based Materials: A Review. Journal of Building Engineering, Vol. 50, Pp.1-17. https://doi.org/10.1016/j.jobe.2022.104220.